Published in final edited form as:
*Nanoscale*. 2014 March 21; 6(6): 3335–3343. doi:10.1039/c3nr06049g.

# A Reversible Light-Operated Nanovalve on Mesoporous Silica Nanoparticles

**Derrick Tarn**[†], **Daniel P. Ferris**[†,‡], **Jonathan C. Barnes**[‡], **Michael W. Ambrogio**[‡], **J. Fraser Stoddart**[‡], and **Jeffrey I. Zink**[†]

[†]Department of Chemistry and Biochemistry, California NanoSystems Institute, University of California, Los Angeles, California 90095, United State

[‡]Department of Chemistry, Northwestern University, 2145 Sheridan Road, Evanston, Illinois 60208-3113

## Abstract

Two azobenzene α-cyclodextrin based nanovalves are designed, synthesized and assembled on mesoporous silica nanoparticles. When in aqueous conditions, the cyclodextrin cap is tightly bound to the azobenzene moiety and capable of holding back loaded cargo molecules. Upon irradiation with a near-UV light laser, *trans* to *cis*- photoisomerization of azobenzene initiates a dethreading process, which causes the cyclodextrin cap to unbind followed by the release of cargo. The addition of a bulky stopper group to the end of the stalk allows this design to be reversible; complete dethreading of cyclodextrin as a result of unbinding with azobenzene is prevented as a consequence of steric interference. As a result, thermal relaxation of cis- to trans-azobenzene allows for the rebinding of cyclodextrin and resealing of the nanopores, a process which entraps the remaining cargo. Two stalks were designed with different lengths and tested with alizarin red S and propidium iodide. No cargo release was observed prior to light irradiation, and the system was capable of multiuse. On / off control was also demonstrated by monitoring the release of cargo when the light stimulus was applied and removed, respectively.

## Introduction

Mesoporous silica has found its application in many fields of chemistry.[1] A subset of mesoporous silica is the MCM-41 type mesoporous silica nanoparticle (MSN), which is characterized by its ordered, 2D hexagonal pore structure.[2] Since its discovery by Mobil researchers several decades ago,[3] MCM-41 has been an ideal choice as a drug delivery platform for its robust nature, high surface area to volume ratio, facile surface modification, low toxicity and high rates of cell internalization.[4] To be an effective drug delivery system, MSNs must be able to retain cargo molecules while in storage and in circulation, but capable of delivering their payload upon arriving at its target. A variety of methods have been employed to prepare MSN to meet these criteria; researchers have exploited hydrophobicity



Correspondence to: Jeffrey I. Zink.

[†]Electronic Supplementary Information (ESI) available: [details of any supplementary information available should be included here]. See DOI: 10.1039/b000000x/

as a method of passive cargo retention,[5] and/or engineered nanomachines based on supramolecular nanovalves,[6a–c] snap-tops,[6d] metal nanocrystals,[6e–f] nanoimpellers,[6g] supported lipid bilayers,[6h] biomolecules,[6i] and reversible chelation[6j] towards the goal of retaining cargo inside the pores of MSN. These systems have been designed to deliver their payload in response to a variety of stimuli; some of which may already be present inside the cell, or is externally applied in the form of magnetic fields[7] and light.[8] The use of internal stimuli such as pH or enzyme activation allows for the creation of a self-contained delivery system, however, they can inevitably lead to higher rates of undesired activation. The use of external stimuli such as light[9] can allow for an additional degree of control through selective irradiation of the target site. Current designs adopt an all-or-nothing type of release: once initiated by a stimulus, cargo is continuously released until the nanocarrier is emptied. While a complete delivery of cargo may sometimes be desired, an alternative approach is to create a nanocarrier capable of delivering its payload in controllable doses. In this way, a single treatment with such nanocarriers can deliver a range of therapeutic concentrations based on the external activating stimulus. To achieve this level of control, a system must be designed that is capable of resealing itself when a particular stimulus is removed. In the case of internal stimuli such as pH or enzyme activation, removing the stimulus is not feasible. Therefore, light, an external stimulus, was considered for its facile on / off manipulation.

We have previously reported a nanovalve based on an azobenzene derivative that is light-operated.[8a] Azobenzenes exhibit the property of photoisomerization, where its more stable *trans*- form can be converted into *cis*-azobenzene through light irradiation of the π -> π* band. Thermal relaxation of *cis*-azobenzene regenerates the *trans*- isomer.[10] This transformation results in a large change in dipole moment; as a result, *cis*-azobenzene is relatively more hydrophilic than the *trans*- conformation. This property allows macrocycles which possess hydrophobic interior regions to selectively bind with *trans*-azobenzene. In the previously reported pseudorotaxane design, light irradiation of an α-cyclodextrin / azobenzene adduct causes the more stable *trans*-azobenzene to isomerize into *cis*-azobenzene. Due to the low binding affinity of α-cyclodextrin towards *cis*-azobenzene, the α-cyclodextrin unthreads from the stalk and allows the cargo to be released. Thermal-relaxation of *cis*-azobenzene back to *trans*- theoretically allows α-cyclodextrin to rebind, but is highly improbable due to the low cap concentration in the media. Therefore, to hold the α-cyclodextrin in proximity to the particle even after it dissociates from the azobenzene, a full rotaxane design was utilized. This allows for recomplexation after thermal conversion back to *trans*-azobenzene, producing a resealing system upon removal of light. Building on our previous azobenzene / β-cyclodextrin design, herein we report the (i) design and synthesis of two new azobenzene stalks **3a** and **3b** (Fig. 1) capable of binding α-cyclodextrin, (ii) the assembly of the pseudorotaxane, **FRS1-NHS** or **EXT2-NHS**, onto MSNs to synthesize the full rotaxane nanovalve, **FRS1-MSN** or **EXT2-MSN**), (iii) the delivery of three different sized fluorescent dyes (alizarin red S (ARS), propidium iodide (PI) and Hoechst 33342) as a result of near-UV light irradiation which allows α-cyclodextrin to slide away from the pore openings, and (iv) the capability of this design to reseal their cargo after the light irradiation is turned off, which allows for dosage control.

## 2. Experimental

### 2.1. General Methods

All of the chemicals used in this study were used as purchased from major suppliers such as Sigma-Aldrich and Fisher Scientific. Release profiles were generated using a time-resolved fluorescence spectroscopy setup (Fig. S12). A Coherent 377 nm CUBE laser was used as the probe beam (1–15 mW, 1 mm diameter), and the emission spectra were monitored using a Princeton Instruments Roper CCD detector cooled to −127 K. The pump beam used was a Coherent 403 nm CUBE laser (1–100 mW, 1 mm diameter) with a manually operated shutter. Powder X-ray diffraction measurements were made using a Panalytical X'Pert Pro diffractometer. All $^{1}$H NMR was performed on a Bruker ARX400 spectrometer in chloroform-d or DMSO-d solvents (400 MHz). Chemical shift is listed in ppm. The solvent signal was used as an internal standard. TEM images were acquired on a JEM1200-EX microscope. TOF-ESI$^{+}$ spectra were collected on a Waters LCT Premier XE Time of Flight instrument. DLS readings were collected on a ZetaPals DLS and zeta potential instrument.

### 2.2. Synthesis of MCM-41 Nanoparticles

Cetyltrimethylammonium bromide (CTAB, 0.25 g, 0.7 mmol) was dissolved in deionized water (120 mL) with heat and stirring. The stir speed and temperature (80 °C) was allowed to stabilize for 1 hour, and then NaOH (2 M, 870 μL, 1.7 mmol) was added to the mixture. To this mixture, triethoxysilane (TEOS, 1.2 mL, 5.4 mmol) was then added drop wise under vigorous stirring (800 RPM) and reacted for 2 hours at 80 °C. The particle suspension was cooled to room temperature, and collected by centrifugation (7830 RPM, 15 min). The collected nanoparticles were washed with methanol until the effluent was a pH of 7. Synthesized nanoparticles showed a monodisperse DLS reading and low PDI (224 nm, PDI 0.01). Pore structure and particle morphology were verified using TEM and XRD, respectively (Fig. S1, S2).

### 2.3. Synthesis of 3-Aminopropyltriethoxysilane Modified MSN

Synthesized MSNs (50 mg) were washed twice with toluene before being resuspended in anhydrous toluene (10 mL). After purging a round bottom flask with dry argon, the reaction vessel was charged with the MSN / toluene slurry and 3-aminopropyltriethoxysilane (30 μL, 0.13 μmol) was added. The mixture was refluxed under dry argon atmosphere for 12 hours, before isolating the nanoparticles via centrifugation (5000 RPM, 5 min). The modified nanoparticles were washed twice with toluene and with DMF. Successful modification of MSN was verified after surfactant extraction with FTIR spectroscopy, as shown in the appearance of two primary amine stretching peaks at 3200 cm$^{-1}$, 3400 cm$^{-1}$ and the appearance of sp$^{3}$ hybridized C–H stretching at 2980 cm$^{-1}$.

### 2.4. Extraction of Templating Agent

MSNs (120 mg) were suspended in a solution of ammonium nitrate in ethanol (133 mg in 50 mL). The mixture was stirred under reflux for 2 hours. The particles were recollected by centrifugation (7830 RPM, 15 min) and washed with methanol (5 × 2 mL). To verify complete extraction of CTAB from the pores, FTIR spectroscopy was performed on the

isolated particles (Fig. S3). DLS readings after surfactant extraction indicated a monodispersed MSNs (180 nm, PDI 0.005).

### 2.5. Synthesis of 4,4′-Azobenzenecarboxylic Acid

*P*-nitrobenzoic acid (15 g, 9 mmols) was dissolved in an aqueous solution of sodium hydroxide (50 g in 225 mL). In a separate reaction vessel, a glucose solution was prepared (100 g, 55 mmols) in water (150 mL) by heating until homogenous. After cooling to room temperature, the glucose solution was added dropwise to the dissolved *p*-nitrobenzoic acid at a rate in order to maintain a temperature of 60 °C and stirred at room temperature for 12 hours under atmospheric oxygen. After the allotted reaction time, the dark brown colored mixture was aged for four hours before filtering. The bright orange precipitate was dissolved in water (50 mL) and acidified with acetic acid (10%, 10 mL) producing a light orange precipitate. After filtering, the product was washed with portions of purified water (3 × 50 mL) and dried under vacuum to yield 4,4'-azobenzenedicarboxylic acid. $^{1}$H NMR (DMSO-$d_6$): δ 7.99 (d, 4H), δ 8.13 (d, 4H).

### 2.6. Synthesis of 2

4,4′-Azobenzenedicarboxylic acid (300 mg, 1.1 mmols) was dissolved in anhydrous DMF (30 mL) with heating. After cooling to room temperature, *N*-hydroxysuccinimide (300 mg, 2.6 mmols) was added to the reaction mixture along with 1-ethyl-3-(3-dimethylaminopropyl)carbodiimide (EDC, 500 mg, 3.2 mmols). A catalytic amount of 4-dimethylaminopyridine (DMAP) was added to the mixture and reacted for 12 hours at room temperature under dry nitrogen. After complete reaction, water (100 mL) was added to the reaction vessel, precipitating out a red solid. After filtering, the product was washed with portions of water (3 × 50 mL) and methanol (30 mL) and vacuum dried to yield a dark red powder. $^{1}$H NMR (DMSO-$d_6$): δ 8.32 (d, 4H), δ 8.14 (d, 4H), δ 2.89 (s, 8H).

### 2.7. Synthesis of 1-Adamantanecarbonyl Chloride

1-Adamantanecarboxylic acid (2 g, 11 mmol) was dissolved in DCM (50 mL) and a catalytic amount of DMF was added before cooling to 0 °C. To this mixture, oxalyl chloride (1.5 mL, 18 mmol) was introduced dropwise. After the dropwise addition, the reaction was allowed to warm to room temperature and reacted for an additional two hours. Completion of the reaction was verified by TLC, and the solvent was removed under reduced pressure to isolate adamantanecarbonyl chloride. The white solid was used without further purification. $^{1}$H NMR (DMSO-$d_6$): δ 2.09 (s, 3H), δ 1.98 (d, 6H), δ 1.78 (q, 6H).

### 2.8. Synthesis of 2b

Potassium carbonate (600 mg) was vacuum dried with heating for 30 minutes and purged with dry argon before adding anhydrous DCM (20 mL) and 2,2′-(ethylenedioxy)bis(ethylamine) (1.5 mL, 10 mmol) (2,2'-EDBEA). The reaction vessel was sealed before cooling to 0 °C in an ice bath. In a separate container, adamantanecarbonyl chloride (1 g, 5 mmol) was dissolved in anhydrous DCM (10 mL) and cooled to 0°C before adding dropwise to the first mixture. After the complete addition, the reaction mixture was allowed to warm to room temperature and stirred for an additional 2 hours, where TLC

analysis confirmed reaction completion. The mixture was filtered to remove excess potassium carbonate, washed once with water (10 mL) and then acidified with hydrochloric acid (10%, 2 mL) before extracting the organic phase with water (3 × 15 mL). The combined aqueous layers were washed with DCM (3 × 10 mL) before adjusting to pH 8 with NaOH (10%). The aqueous layer was then extracted with DCM (5 × 15 mL), and the combined organic layers washed with brine, and dried under anhydrous sodium sulfate before concentrating under rotary evaporator to yield compound **2b** as a viscous, clear liquid. $^{1}$H NMR (chloroform-d): δ 6.13 (s, 1H), δ 3.53 (s, 4H), δ 3.42 (m, 4H), δ 3.29 (q, 2H), δ 2.74 (t, 2H), δ 1.90 (s, 3H), δ 1.72 (s, 6H), δ 1.57 (t, 6H). TOF-ESI$^{+}$ MS (calculated at 310.2): m/z 311.2 (M+H$^{+}$).

### 2.9. Synthesis of 3a

In a reaction vessel, compound **2** (100 mg, 0.22 mmols) was dissolved in DMF (20 mL) with gentle heating and cooled to room temperature. Separately, adamantylamine (50 mg, 0.33 mmols) was dissolved in anhydrous DCM (5 mL) and cooled to 0 °C. The adamantylamine mixture was added to the mixture containing compound **2** dropwise over 2 hours, and allowed to react overnight at room temperature. After completion, the mixture was diluted with water (50 mL) and extracted with ethyl acetate (3 × 30 mL). The organic phases were combined and washed with water (5 × 20 mL) to remove the dissolved DMF, washed with brine and dried with anhydrous sodium sulfate. After concentrating the solution under reduced pressure, the crude product was purified with column chromatography on a silica stationary phase (EtOAc : hexanes = 1 : 2), and the second band isolated to yield quantitative amounts of **3a**. $^{1}$H NMR (DMSO-$d_6$): δ 8.29 (d, 2H), δ 8.09 (d, 2H), δ 7.95 (m, 4H), δ 2.89 (s, 4H), δ 2.24 (t, 3H), δ 2.05 (d, 6H), δ 1.64 (s, 6H). TOF-ESI$^{+}$ MS (calculated at 500.2): m/z 501.2 (M+H$^{+}$).

### 2.10. Synthesis of 3b

In a round bottom flask, compound **2** (100 mg, 0.22 mmols) was dissolved in DMF (20 mL) with gentle heating and allowed to cool to room temperature. In a separate vessel, compound **2b** (100 mg, 0.32 mmols) was dissolved in DCM (5 mL) before adding to the solution of compound **2** over a period of 2 hours. After the complete addition, the mixture was allowed to react overnight at room temperature before diluting with water (30 mL) and extracting with ethyl acetate (5 × 10 mL). The combined organic layers were washed with water (5 × 15 mL), once with brine and dried over anhydrous sodium sulfate before concentrating on a rotary evaporator. The crude product was purified with column chromatography on a silica stationary phase, and eluted with ethyl acetate. The second band was isolated as a dark red solution, and the solvent evaporated under reduced pressure to isolate **3b** as a dark red powder. $^{1}$H NMR (chloroform-d): δ 8.31 (d, 2H), δ 7.97–8.05 (m, 6H), δ 6.87 (s, 1H), δ 5.97 (s, 1H), δ 3.58–3.72 (m, 8H), δ 3.57 (t, 2H), δ 3.44 (q, 2H), δ 2.94 (s, 4H), δ 2.01 (s, 3H), δ 1.82 (d, 6H), δ 1.67 (s, 6H). TOF-ESI$^{+}$ MS (calculated at 659.3): m/z 660.3 (M+H$^{+}$).

### 2.11. Synthesis of FRS1-NHS

**3a** (6 mg, 1.1 μmol) and α-cyclodextrin (17 mg, 2.3 μmols) were dissolved in anhydrous DMF (1 mL). The reaction mixture was stirred at room temperature for an additional 2 hours to form pseudorotaxane **FRS1-NHS**.

### 2.12. Synthesis of EXT2-NHS

**3b** (2 mg, 0.3 μmols) and α-cyclodextrin (6 mg, 0.7 μmols) were added and dissolved in anhydrous DMF (1 mL). The reaction mixture was also stirred at room temperature for an additional 2 hours to allow α-cyclodextrin to thread onto **3b** to synthesize pseudorotaxane **FRS1-NHS**.

### 2.13. Synthesis of FRS1-MSN

APTES-modified MSNs (20 mg) were washed twice with DMF before being resuspended in a mixture of **FRS1-NHS** (23 mg in 1 mL DMF). The reaction vessel was sealed under dry argon atmosphere and allowed to react for 12 hours at room temperature, before collecting through centrifugation (15000 RPM, 3 min). The stalk modified nanoparticles were washed with two portions of methanol and resuspended in ethanol. Successful attachment of the stalk was verified through UV-Vis spectroscopy of a suspension of **FRS1-MSN** (Fig. S10).

### 2.14. Synthesis of EXT2-MSN

A sealed reaction vessel purged with dry argon gas was charged with APTES-modified MSN (20 mg) that have been washed twice with anhydrous DMF. To this, a solution of **EXT2-NHS** (8 mg in 1 mL DMF) was added and allowed to react at room temperature for 12 hours. The product was collected through centrifugation (15000 RPM, 3 min), washed twice with methanol and suspended in ethanol. Successful attachment of the stalk was verified through UV-Vis spectroscopy of a suspension of **EXT2-MSN** (Fig. S11)

### 2.15. Loading of Fluorescent Dye and Sealing in Cargo

A sample of **FRS1-MSN** or **EXT2-MSN** was suspended in a concentrated dye solution. For the ARS loaded samples, the nanoparticles were suspended in an ethanoic ARS dye solution (2 mM, 1 mL). For Hoechst 33342 samples, the nanoparticles were suspended in a solution of Hoechst in ethanol:acetone = 1:1 (1 mmol, 1 mL). For PI loaded samples, **EXT2-MSN**s were suspended in an ethanoic PI dye solution (1 mM, 1 mL). Samples were stirred at room temperature for 24 hours before collecting with centrifugation (15000 RPM, 10 min). To seal in cargo and wash off excess surface-adsorbed dye, samples were washed with water until the supernatant exhibited no more fluorescence under 365 nm light and dried under vacuum prior to testing.

### 2.16. Assessment of Light activated Cargo Release

**FRS1-MSN** or **EXT2-MSN** (5 mg) loaded with an appropriate dye were confined to the corner of a glass cuvette. Water (4 mL) was gently added to the particles at a rate to prevent particles from being resuspended into solution. A 377 nm excitation laser (1 mW) was aimed through the solution supernatant. Emission of dye molecules released from each sample in the solution supernatant was monitored in real time by focusing the emitted light

through a collecting lens, a 450 nm cutoff filter, and a monochromator (300 nm window) before integrating on a CCD detector (Fig. S12). To track release of ARS, the monochromator was centered on 550 nm, and the fluorescence integrated from 550–600 nm. PI release was monitored by centering the window at 600 nm and tracking dye emission from 600–620 nm. A baseline was collected over 1.5 hours to allow solution suspended particles to settle before a 403 nm pump beam (85 mW) was focused directly on the sample to stimulate cargo release. For the on/off experiments, the pump beam was turned off at timed intervals.

### 2.17. Reloading and Reuse Assessment

After acquiring a complete release profile, the sample was heated to 60 °C in ethanol for 12 hours in order to release the cargo from any particles that may not have been exposed to the irradiating laser. The solution was centrifuged (15000 RPM, 15 min) to remove suspended nanoparticles and analyzed under UV-Vis spectroscopy in order to verify the identity of the released cargo, and the sample pellet reloaded in an appropriate dye solution before washing away the unloaded excess. The reloaded samples were subjected to a second release profile test, and the corresponding time resolved fluorescence spectra collected in a similar fashion as described above.

## 3. Results and Discussion

### 3.1. Design of the Nanovalves

For adequate functioning of the nanovalve, a stalk must be designed that exhibits regional, reversible binding with a nanocap. After threading the nanocap with the stalk and assembling the 1:1 complex on the surface of the nanoparticle, the “closed” state of the stalk, the region of highest affinity, brings the nanocap close enough to the particle surface to prevent escape of the cargo. When binding is no longer favorable, the nanocap slide along the stalk away from the surface of the nanoparticle to its “open” state before reaching an end-terminating stopper group. This allows the cargo molecules to diffuse from the pores, but prevents the nanocap from unthreading completely. To achieve light responsiveness, the binding affinity of the capping agent must also be light dependent. For this reason, building on the previously designed pseudorotaxane azobenzene-cyclodextrin motif, an azobenzene moiety was chosen.

Similarly to the pseudorotaxane design,8[a] in the dark, the α-cyclodextrin can bind and form a supramolecular complex with the *trans*-azobenzene moiety, which is driven by favorable interactions between the hydrophobic α-cyclodextrin cavity and the azobenzene core.[11] While all of the cyclodextrins exhibit a respectable binding affinity with *trans*-azobenzene, α-cyclodextrin was chosen for its ideal size in having an inner cavity diameter of 0.47 nm on the primary face and 0.53 nm on the secondary face.[12] Irradiating with light causes *trans*-azobenzene to isomerize into its *cis*- form, which, due to its increased hydrophilicity, no longer has a favorable binding affinity with α-cyclodextrin and results in translation of the nanocap along the stalk. Although the α-cyclodextrin is able to slide along the stalk, after irradiation, complete dethreading is prevented by incorporating a stalk-terminating stopper group.

Several requirements for the choice of a stopper group were considered. The stopper must simultaneously be bulky enough to prevent the α-cyclodextrin from unthreading, but also have a lower binding affinity with α-cyclodextrin than *trans*-azobenzene in order to limit competitive binding with the stopper. For these reasons, an adamantane functional group was selected as the stopper. This molecule, with a diameter of 0.5 nm, is large enough to prevent α-cyclodextrin from unthreading, while exhibiting a low binding affinity for the nanocap. While other members of the cyclodextrin family –namely, β- and γ-cyclodextrin– have binding constants of 7000 $M^{-1}$ and 3500 $M^{-1}$ with adamantane,[13a] respectively, the strength of the α-cyclodextrin / adamantane adduct is considerably weaker by an order of magnitude (100 $M^{-1}$).[13] In this way, α-cyclodextrin will preferentially bind *trans*-azobenzene, but in the case when only *cis*-azobenzene forms by photoexcitation, the nanocap forms a metastable adamantane / α-cyclodextrin state that holds the nanocap away from the pore openings to allow release of the cargo. To ensure an adequate spatial clearance for cargo movement during this event, the distance between the azobenzene moiety and end stopper must be carefully tailored.

Because the size of many chemotherapy drugs falls between 1 – 2.5 nm, we designed two stalks of different lengths in order to load and deliver both 1 nm and 2 nm sized cargo molecules. To illustrate this, three fluorescent dyes: alizarin red S (ARS), propidium iodide (PI), and Hoechst 33342 with diameters 1.2 nm, 1.8 nm and 2.0 nm, respectively, were chosen as the cargo molecules (Fig. 2a). **FRS1-MSN** was tailored so that its “open” state could to allow for movement of cargo with sizes up to 1.6 nm, whereas in its “closed” state, the clearance is reduced to 0.8 nm (Fig. 2b-left). Therefore, ARS was selected as a candidate to test **FRS1-MSN** since it is 1.2 nm in size. **EXT2-MSN** was designed with a 2.8 nm “open” distance when fully extended (Fig. 2b-right). Similarly to **FRS1-MSN**, in its closed conformation, **EXT2-MSN** reduces the α-cyclodextrin-to-pore distance to 0.8 nm in order to seal the mesopores. As such, stalk **FRS1-MSN** is expected to load and deliver ARS but fail with PI or Hoechst, and stalk **EXT2-MSN** is expected to be compatible with PI.

### 3.2. Synthesis of MSNs

MSNs were synthesized utilizing a surfactant-templated sol-gel process.[14] The resulting spherical nanoparticles were ~100 nm in diameter. After synthesis, MSN was directly modified with 3-aminopropyltriethoxysilane (APTES) by a condensation reaction with the surface silanol groups in order to bias modification to the nanoparticle surface and prepare for subsequent stalk attachment. After modification with APTES, removal of the templating agent resulted in nanoparticles with hexagonally arranged mesopores about 2.2 nm in diameter (Fig. S1–S3).

### 3.3. Synthesis of the Stalks

Since α-cyclodextrin / azobenzene binding is dependent on hydrophobic interactions, considerations in the synthesis of both stalks were made to ensure that the final attachment steps onto MSN could be made in a polar solvent. Because of this, a NHS ester functional group was chosen as the reactive end for its specificity and compatibility with non-aqueous, polar solvents. In the synthesis of both stalks, *p*-nitrobenzoic acid was reacted in basic conditions with glucose to form compound **1**. To generate the di-substituted NHS ester

product, **1** was reacted with N-hydroxysuccimide to form **2**. To prepare the short stalk, **2** was directly reacted with adamantylamine (**2a**) under dilute conditions and purified via column choromatography to isolate the monosubstituted product **3a**. To prepare the long stalk, first, adamantanecarboxylic acid was reacted with oxalyl chloride to generate adamantane carbonyl chloride. Then, nucleophilic substitution of the acid chloride with 2,2'-(ethylenedioxy)bis(ethylamine) afforded the monoalkylated product **2b**. **2b** was reacted with **2** under dilute conditions and purified under column chromatography to yield the longer stalk **3b**. To synthesize the pseudorotaxane, compounds **3a** or **3b** were mixed with α-cyclodextrin in DMF to allow α-cyclodextrin to complex with azobenzene and form the pseudorotaxanes **FRS1-NHS** and **EXT2-NHS**, respectively. Attachment to MSNs was accomplished by first modifying MSNs with 3-aminopropyltriethoxysilane and extracting the templating agent before a direct reaction with **FRS1-NHS** or **EXT2-NHS** to complete the synthesis of **FRS1-MSN** or **EXT2-MSN**.

### 3.4. Loading and Sealing of Cargo

After grafting each of the pseudorotaxane stalks onto MSNs, the assembled machines were washed with methanol to remove unreacted excess material. In order to load cargo into the pores, **FRS1-MSN** or **EXT2-MSN** were suspended in an organic solvent under UV light irradiation to break the hydrophobic interactions between α-cyclodextrin and azobenzene to allow α-cyclodextrin to slide toward the adamantane end and allow for pore access (Fig. 2c–3). Suspending and stirring the nanoparticles in an organic solution of fluorescent dye allowed cargo to slowly load inside the pores. In order to seal the nanocap, the loaded nanoparticles were solvent exchanged with water, where the exclusion of solvent from the cyclodextrin cavity is favored, allowing the α-cyclodextrin cap to rebind with azobenzene and reseal tightly the loaded cargo (Fig. 2c–4). Excess, surface-adsorbed cargo was removed with subsequent water washes until the eluent no longer exhibited fluorescence.

### 3.5. Characterization

The MSN quality was determined through TEM imaging (Fig. S1), which confirmed an average diameter of 100 nm and a 2D-hexagonally packed pore structure with pore diameters of 2–2.4 nm. Powder XRD measurements (Fig. S2) were used to confirm the hexagonal mesopore phase, evident in the higher order Bragg diffraction peaks indexed as the (100), (110), and (200) planes with a lattice spacing of 4 nm. Complete removal of CTAB was verified by subjecting bare MSN to the extraction procedure and performing FTIR spectroscopy (Fig. S3) on the resulting material, which showed a complete removal of organic material with the disappearance of $sp^3$ C-H stretching peaks present around 3000 $cm^{-1}$. Successful amine modification of MSN was verified through FTIR spectroscopy, with the appearance of the dual primary amine stretches around 3200 $cm^{-1}$ and $sp^3$ C-H stretching peaks at 3400 $cm^{-1}$ after CTAB extraction. To verify the success of each step in the synthesis of **3a** and **3b** $^1$H NMR and ESI-TOF mass spectrometry were employed (Fig. S4–S8) on each of the intermediates in the stalk syntheses. The attachment efficiency of both **FRS1-NHS** and **EXT2-NHS** pseudorotaxanes to MSN was verified through UV-Vis spectroscopy,. **FRS1-MSN** and **EXT2-MSN** showed similar absorption peaks centered at 334 and 336 nm respectively, which can be attributed to a successful attachment of the

azobenzene stalks (Fig. S9–S10). After isolating the modified nanoparticles through centrifugation, absorption spectroscopy of the corresponding supernatant showed a negligible absorbance in this region, which indicates the attachment process was highly efficient.

### 3.6. Light Activated Cargo Delivery

To verify the operation of the nanomachine, continuous monitoring by fluorescence spectroscopy was employed. In a corner of a quartz cuvette, a dried sample of **FRS1-MSN** or **EXT2-MSN** was confined and water gently added in order to prevent suspending the nanoparticles into solution. To monitor the release of cargo, a low power probe beam (377 nm, 1 mW) was aimed through the solution supernatant in order to excite the fluorescent dye molecules released from the sample. The corresponding emission was filtered through a cut-off filter and selected using a monochromator before focusing onto a CCD detector. Integrating over a specific range of wavelengths in real-time allowed for the generation of a time-resolved release profile. In order to irradiate the sample and induce cargo release, a pump beam (403 nm, 85 mW, 1 mm diameter), was directly focused onto the sample.

### 3.7. FRS1-MSN Light Activated Release

Using a time resolved spectroscopy technique (Fig. S12), an initial baseline reading of the **FRS1-MSN** sample was collected for two hours. Fig. 3a shows no dye release prior to activation of the pump beam, illustrating the strength of the α-cyclodextrin / *trans*-azobenzene complexation in sealing off the cargo. When irradiated, an increasing ARS fluorescence is observed (Fig. 3a–1), indicating the release of cargo. The curved shape illustrates an initially high release rate as dye molecules diffuse from the highly concentrated pore interiors into the solution. After several hours, the slope of the curve flattens out as fewer dye molecules remain inside the pores. To demonstrate the reusability of the rotaxane valve, after a completed release, the sample was washed with ethanol to remove any remaining dye, reloaded with ARS, and washed in water to remove surface adsorbed-dye and reseal the pores. This reloaded sample was subjected to the same release profile experiment to ensure that α-cyclodextrin is still present on the rotaxane stalk and capable of sealing in cargo. The baseline in Fig. 3a–2 demonstrates that this reloaded sample remains tightly sealed prior to light irradiation, indicating that the nanocap has not been removed from the rotaxane stalk. After irradiation with the pump laser, an increase in ARS fluorescence is observed, showing that the system is still light responsive, and suggesting the reusability of **FRS1-MSN**. To confirm the observed fluorescence change is due to ARS, the supernatant was analyzed (Fig. S11) after each release profile using UV-Vis spectroscopy and compared to a standard solution of ARS.

In order to also verify the reversibility of the rotaxane nanovalve, **FRS1-MSN** was subjected to a series of “on” / “off” tests. In the same experimental setup as described above, cargo release from a **FRS1-MSN** sample loaded with ARS was tracked while the pump beam was turned off for 30 minute intervals (Fig. 4a). At first, when irradiated, **FRS1-MSN** exhibits the presumed exponential shape indicative of ARS release, but flattens out when the pump beam is turned off. This can be attributed to a thermal relaxation of *cis*-azobenzene into *trans*-azobenzene in the dark, which allows α-cyclodextrin to rebind and prevent additional

cargo release. Reintroducing the pump beam to the sample causes ARS fluorescence to increase once more, indicating the reversibility of this system and its potential for dosage control.

In order to ensure the necessity of α-cyclodextrin in the rotaxane design, a control experiment was performed in which a sample of **3a** was assembled without first threading on α-cyclodextrin to produce **FRS1-MSN**. This sample was then loaded with ARS and washed until the supernatant was colorless. The corresponding fluorescence release profile was also acquired with this sample, which showed increasing ARS fluorescence prior to pump beam irradiation. This suggests that without a cyclodextrin cap, the azobenzene stalk alone is unable to retain cargo molecules (Fig. 4b), and thus demonstrates the necessity of the α-cyclodextrin nanocap for successfully sealing in ARS cargo.

Although **FRS1-MSN** is able to load and release ARS, the dimensions of these nanoparticles in their closed and open states indicate that it is unable able to load cargo greater than 1.5 nm. To test this, **FRS1-MSN** was assembled and loaded with Hoechst 33342 (diameter =2 nm). After the loading and washing steps, the loaded nanoparticles were not fluorescent under a UV-lamp, indicating that Hoechst was not able to access the pores of the **FRS1-MSN**. To corroborate this, the sample was tested in a release profile experiment while monitoring the solution for Hoechst fluorescence. After collecting a baseline, irradiating the sample with the pump laser caused no change in fluorescence over the background noise (Fig. S13). Because of its length, **FRS1-MSNs** are unable to load a larger sized cargo molecule like Hoechst. The longer stalk length of EXT2 allows cargo up to 2.2 nm to be loaded inside of the pores. To assess whether this longer design can achieve the goal of delivering larger cargo molecules, stalk EXT2 was tested similarly with PI as the fluorescent cargo molecule.

### 3.8. EXT2-MSN Light Activated Release

Using the same laser based time-resolved spectroscopy techniques, **EXT2-MSN** was tested as a delivery system for PI cargo. In order to detect PI emission, the monochromator was centered at 600 nm with a 300 nm window. Similarly, a baseline reading was collected before activating the pump beam and stimulating cargo release. Prior to activating the pump beam, the initial flat baseline reading for **EXT2-MSN** (Fig. 3b–1) shows no observable PI fluorescence, showing that this rotaxane stalk is capable of sealing in the PI cargo. When the pump beam is turned on, an increase in fluorescence is observed, indicating that PI is being released from the nanoparticles and into the solution. The solution fluorescence of PI increases gradually over several hours before approaching completion, when the dye has been completely released from **EXT2-MSN**. This experiment indicates that **EXT2-MSN** is capable of releasing PI dye with light stimulation.

In order to verify that light irradiation did not destroy the stalk, or cause α-cyclodextrin to unthread altogether, after a completed release the sample was washed to remove any remaining PI cargo before reloading in a fresh solution of PI. After washing off the excess, surface adsorbed dye with water, a second release profile was generated under the same conditions as used previously (Fig. 3b–2). The initial collection of data shows a flat baseline prior to pump beam activation, indicating that the reloaded **EXT2-MSN** system is still

capable of sealing in PI. Upon irradiation with the pump beam, an increase in solution fluorescence is observed, suggesting that PI cargo is again diffusing from the nanoparticle pores and into the solution. Because the reloaded cargo releases only upon irradiation, **EXT2-MSN** is observed to be a reusable, light-responsive delivery system for PI.

## 4. Conclusions

In summary, two reversible, reusable nanovalves were designed based on the azobenzene / α-cyclodextrin recognition motif that is capable of the controlled release of both small cargo (ARS dye) and larger dye molecules (PI). In aqueous environments, both nanovalves remain tightly closed due to the strong binding between α-cyclodextrin and the *trans*-azobenzene moiety, but light irradiation causes the photoisomerization of *trans*- to *cis*-azobenzene, unbinding the α-cylodextrin cap and allowing it to slide to the adamantane end of the stalk, which results in the release of the cargo. Because this binding is reversible, once the light is turned off, thermal relaxation of *cis*-azobenzene regenerates *trans*-azobenzene, which allows the cyclodextrin to rebind and seal in the remaining cargo molecules. By tuning the length of the azobenzene / adamantane stalk, cargo size-selectivity can be achieved. Currently, this system is being tested *in-vitro* with the goal of developing an externally light-activated nanovalve to deliver anti-cancer drugs to cancerous cells.

## Supplementary Material

Refer to Web version on PubMed Central for supplementary material.

## Acknowledgements

The project described was supported by Grant Numbers S10RR025631 from the National Center for Research Resources and CA133697 from the National Institutes of Health. Support from the U.S. Department of Defense and from the Northwestern University International Institute for Nanotechnology is also acknowledged.

## Notes and references

1. (a) Lu Y, Ganguli R, Drewien CA, Anderson MT, Brinker CJ, Gong W, Guo Y, Soyez H, Dunn B, Huang MH, Zink JI. Nature. 1997; 389:364–368.(b) Slowing II, Trewyn GB, Giri S, Lin SV. Adv. Funct. Mater. 2007; 17:1225–1236.(c) Zhao D, Feng J, Huo Q, Melosh N, Fredrickson GH, Chmelka BF. Science. 1998; 279:548–552. [PubMed: 9438845] (d) Lin Y-S, Hurley KR, Haynes CL. J. Phys. Chem. Lett. 2012; 3:364–374.(e) Li Z, Barnes JC, Bosoy A, Stoddart JF, Zink JI. Chem. Soc. Rev. 2012; 41:2590–2605. [PubMed: 22216418]
2. Kresge CT, Leonowicz ME, Roth WJ, Vartuli JC, Beck JS. Nature. 1992; 359:710–712.
3. Beck JS, Vartuli JC, Roth WJ, Leonowicz ME, Kresge CT, Schmitt KD, Chu CTW, Olson DH, Sheppard EW. J. Am. Chem. Soc. 1992; 114:10834–10843.
4. (a) Liong M, Lu J, Kovochich M, Xia T, Ruehm SG, Nel AE, Tamanoi F, Zink JI. ACS Nano. 2008; 2:889–896. [PubMed: 19206485] (b) Ambrogio MW, Thomas CR, Zhao Y-L, Zink JI, Stoddart JF. Acc. Chem. Res. 2011; 44:903–913. [PubMed: 21675720] (c) Trewyn BG, Slowing II, Giri S, Chen H-T, Lin VSY. Acc. Chem. Res. 2007; 40:846–853. [PubMed: 17645305] (d) Zhang H, Dunphy DR, Jiang X, Meng H, Sun B, Tarn D, Xue M, Wang X, Lin S, Ji Z, Li R, Garcia FL, Yang J, Kirk M, Xia T, Zink JI, Nel AE, Brinker CJ. J. Am. Chem. Soc. 2012; 134:15790–15804. [PubMed: 22924492] (e) Yanes RE, Tarn D, Hwang AA, Ferris DP, Sherman SP, Thomas CR, Lu J, Pyle AD, Zink JI, Tamanoi F. Small. 2013; 9:697–704. [PubMed: 23152124]
5. Lu J, Liong M, Zink JI, Tamanoi F. Small. 2007; 3:1341–1346. [PubMed: 17566138]

6. (a) Meng H, Xue M, Xia T, Zhao Y-L, Tamanoi F, Stoddart JF, Zink JI, Nel AE. J. Am. Chem. Soc. 2010; 132:12690–12697. [PubMed: 20718462] (b) Angelos S, Yang Y-W, Khashab NM, Stoddart JF, Zink JI. J. Am. Chem. Soc. 2009; 131:11344–11346. [PubMed: 19624127] (c) Li Z, Nyalosaso JL, Hwang AA, Ferris DP, Yang S, Derrien G, Charnay C, Durand J-O, Zink JI. J. Phys. Chem. C. 2011; 115:19496–19506.(d) Coti KK, Belowich ME, Liong M, Ambrogio MW, Lau TA, Khatib HA, Zink JI, Khashab NM, Stoddart JF. Nanoscale. 2009; 1:16–39. [PubMed: 20644858] (e) Vivero-Escoto JL, Slowing II, Trewyn BG, Lin VS-Y. Small. 2010; 6:1952–1967. [PubMed: 20690133] (f) Lai C-Y, Trewyn BG, Jeftinija DM, Jeftinija K, Xu S, Jeftinija S, Lin VS-Y. J. Am. Chem. Soc. 2003; 125:4451–4459. [PubMed: 12683815] (g) Lu J, Choi E, Tamanoi F, Zink JI. Small. 2008; 4:421–426. [PubMed: 18383576] (h) Liu JW, Stace-Naughton A, Jiang XM, Brinker CJ. J. Am. Chem. Soc. 2009; 131:1354–1355. [PubMed: 19173660] (i) Ferris DP, Lu J, Gothard C, Yanes R, Thomas CR, Olsen J-C, Stoddart JF, Tamanoi F, Zink JI. Small. 2011; 7:1816–1826. [PubMed: 21595023] (j) Tarn D, Xue M, Zink JI. Inorg. Chem. 2013; 52:2044–2049. [PubMed: 23391170]
7. Thomas CR, Ferris DP, Lee J-H, Choi E, Cho MH, Kim ES, Stoddart JF, Shin J-S, Cheon J, Zink JI. J. Am. Chem. Soc. 2010; 132:10623–10625. [PubMed: 20681678]
8. (a) Ferris DP, Zhao Y-L, Khashab NM, Khatib HA, Stoddard JF, Zink JI. J. Am. Chem. Soc. 2009; 131:1686–1688. [PubMed: 19159224] (b) Nguyen TD, Leung KC-F, Liong M, Liu Y, Stoddart JF, Zink JI. Adv. Funct. Mater. 2007; 17:2101–2110.
9. (a) Angelos S, Choi E, Vögtle F, De Cola L, Zink JI. J. Phys. Chem. C. 2007; 111:6589–6592.(b) Aznar E, Casasús R, García-Acosta B, Marcos MD, Martínez-Mánaz R, Sancenón F, Soto J, Amorós P. Adv. Mater. 2007; 19:2228–2231.
10. Rabek, JF. Photochemistry and Photophysics. Vol. Volume II. CRC Press, Inc; Boca Raton, Florida: 1990.
11. Murakami H, Kawabuchi A, Kotoo K, Kunitake M, Nakashima NJ. J. Am. Chem. Soc. 1997; 119:7605–7606.
12. Del Valle EMM. Process Biochem. 2004; 39:1033–1046.
13. (a) Falvey P, Lim CW, Darcy R, Revermann T, Karst U, Giesbers M, Marcelis ATM, Lazar A, Coleman AW, Reinhoudt DN, Ravoo BJ. Chem. Eur. J. 2005; 11:1171–1180. [PubMed: 15619722] (b) Cromwell WC, Bystrom K, Eftink MR. J. Phys. Chem. 1985; 89:326–332.
14. Angelos S, Liong M, Choi E, Zink JI. Chem. Eng. J. 2008; 137:4–13.

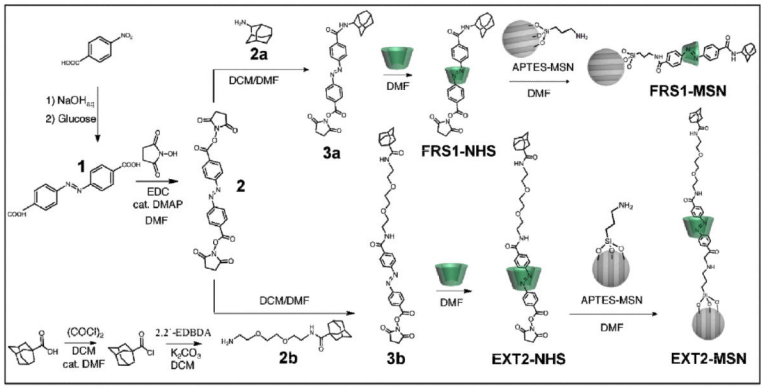


**Fig. 1.**

Schematic overview of the synthesis of **FRS1-MSN** and **EXT2-MSN**; *p*-nitrobenzoic acid is reacted with glucose to give **1**. Reaction with *N*-hydroxysucciminide yields **2**. Monosubstitution of **2** with one equivalent of **2a** or **2b** yields **3a** or **3b**, respectively. Complexation with α-cyclodextrin forms the α-cyclodextrin/azobenzenepseudorotaxanes **FRS1-NHS** or **FRS1-NHS**. Reaction of the pseudorotaxanes with APTES-MSNs yields **FRS1- MSN** or **EXT2-MSN**.

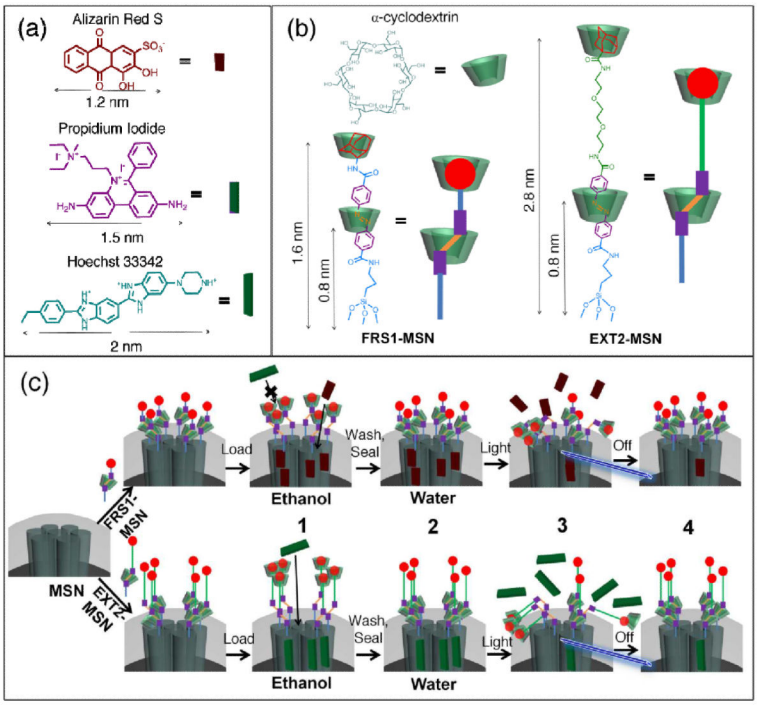


**Fig. 2.**

(a) Size illustration of various cargo molecules in reference to (b) azobenzene stalks **FRS1-MSN** and **EXT2-MSN**. Because of the shorter stalk length, **FRS1-MSN** is limited to loading cargo molecules < 2 nm. Hoechst 33342 and propidium iodide dyes remain excluded from **FRS1-MSN** as a result of their size. However, **EXT2-MSN** is observed to load all three of the listed fluorophores. (c) Schematic illustration of the fully assembled rotaxane nanovalve and operation. (1) After synthesis, the nanovalves are suspended in an organic solvent, which destabilizes hydrophobic interactions between the α-cyclodextrin and azobenzene moiety and allows for cargo loading. (2) Upon solvent exchange to water, rebinding of the cyclodextrin to azobenzene seals in the loaded cargo. (3) Irradiation with light induces isomerization to *cis*-azobenzene, forcing cyclodextrin to move to the end of the stalk, and allowing cargo to release. (4) Upon removal of the light stimulus, thermal relaxation of *cis*-azobenzene to its more stable *trans* isomer allows rebinding of the cyclodextrin and seals in the remaining cargo.

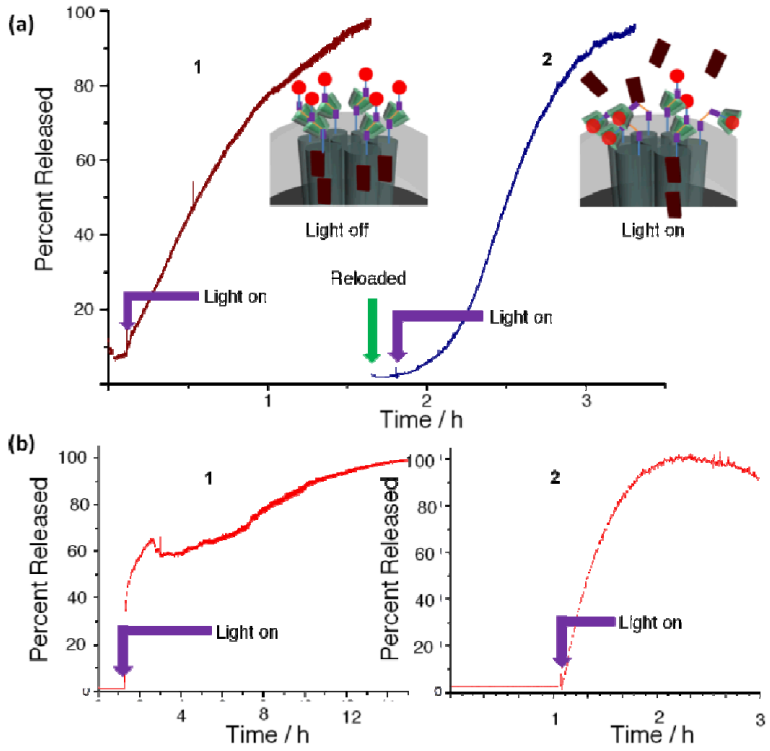


**Fig. 3.**

(a) Time resolved fluorescence spectra showing the light activated (403 nm) release of alizarin red S (ARS) dye from **FRS1-MSN**. Initial loading of the particles results in minimal release prior to irradiation (trace 1). When the pump beam is activated, ARS fluorescence steadily increases in the supernatant. After the release is complete, **FRS1-MSN** were reloaded with ARS and washed before reinitiating cargo release. Trace 2 shows these reloaded **FRS1-MSN** releases ARS equally as well. An identical experiment was performed on the **EXT2-MSN** system (b) using PI dye instead. **EXT2-MSN** exhibits the same behavior as **FRS1-MSN** with the larger fluorophore. These results demonstrate that the full rotaxane systems are reversible, reusable and can bedesigned to release different sized cargos.

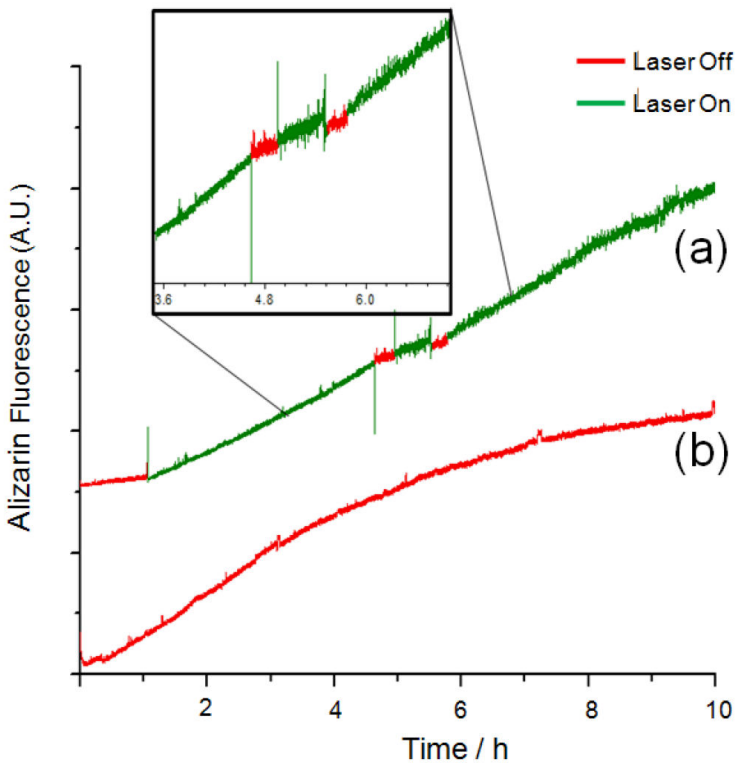


**Fig. 4.**

Time resolved fluorescence spectra demonstrating the on-off properties of **FRS1-MSN**. (a) Stimuli-response release profile; light stimuli causes the release of the ARS. When the light is turned off, the fluorescence intensity levels out until the stimulus is reapplied. (b) Release from the particles modified by 3a rather than **FRS1-NHS**. The stalk, lacking the cyclodextrin nanocap, shows a continuous release of ARS without application of light. Therefore, the α-cyclodextrin is required to form the complete nanovalve system and prevent leakage of cargo.